Chapter 5

Gold-coated electrospun PVA nanofibers as SERS substrate for detection of pesticides

In this chapter, design of SERS substrate has been realized through electrospinning technique. Electrospun PVA nanofibers are coated on a glass substrate followed by Gold (Au) film deposition. Subsequently, the substrate has been used for reliable detection and quantification of three commonly used pesticides through recording and analyzing of scattered Raman signals from the substrate.

5.1 Introduction

SERS is considered to be one of the most sensitive and versatile technique for detection of various biomolecules, different chemicals, toxins, explosives, pesticides, food contaminants, virus, different gases, etc. Different types of SERS substrates have been used for these purposes. The SERS substrates can be obtained by adopting either by wet-chemical method or top-down fabrication method. The substrates obtained from wet-chemical method yields high EF and sensitivity but suffers from poor reproducibility. The latter method can generate highly reproducible SERS substrate, however, such method demands highly sophisticated machines, good laboratory facilities and is a time consuming process. This approach is therefore expensive and can be obtained only after fulfilling several criteria. To overcome these issues, researchers are currently looking for alternative

approaches by which SERS substrates can be obtained at an affordable cost. Substrates can be obtained from naturally available patterned biological samples such as rose petals, diatom frustules, taro leaf, etc [1-5] and some other low-cost techniques such as inkjet and screen printing [6-8]. Obtaining a SERS substrate from diatom frustules and printing grade paper have been discussed in chapter 3 and 4 of this thesis work. These techniques are observed to be cost effective and time-efficient. In this chapter, a technique to obtain SERS substrate from electrospun Poly(vinyl alcohol) (PVA) nanofibers by depositing Au nanofilm on PVA nanofibers has been discussed thoroughly. PVA is a highly hydrophilic, non-toxic and biocompatitible polymer and exhibits excellent physical properties such as strength, water solubility, gas permeability and thermal stability [9-11]. PVA in different form such as nanofilm, nanofiber have been used in cell and tissue culture, cell repairing, LSPR based sensing etc. [12-17]. Owing to its biocompatibility nature, designing of SERS substrate using PVA nanofiber could usher new alternative of research in the field of biosensing. In the present thesis work the performance of the proposed Au coated PVA nanofiber substrate has been evaluated by measuring Raman signal from MG and BPE and subsequently use it for detection of three pesticides largely used in the field of agricultural.

To manage pest problem different types of pesticides have been used in agricultural field. Apart from agricultural fields, pesticides are also used in homes, parks, schools, buildings, forests, and roads. It has been estimated that only 0.1% of applied pesticides could reach the target [18]. The rests are remaining in the environment, which may pollute the environment and then directly or indirectly enter into the food chain. Pesticides are linked to human health hazards ranging from short-term impacts to chronic impacts. Short-term impacts such as headaches and nausea and chronic impacts like cancer, reproductive harm and endocrine disruption could cause due to consumption of pesticides. Acute dangers - such as nerve, skin, eye irritation and damage, headache, dizziness, fatigue and systemic poisoning can sometimes be dramatic, and even occasionally fatal also may be the reason of pesticides consumption. Issues related to chronic health effects may occur years even after minimal exposure to it in the environment or results from the pesticide residues [19-21]. Thus, reliable detection techniques of pesticides contained in various food items at an affordable cost would be a relevant study for healthy and sustainable living style. Techniques such as gas chromatography, mass spectrometry, high-performance liquid chromatography etc. [22-26] are conventional techniques for detection of pesticides. However, these techniques are time consuming. Other techniques such as capillary electrophoresis, UV-Vis spectrometry, immunoassays, SPR based sensing, SERS base detection, electrochemical detection etc. are rapid pesticides detection techniques [27-35]. Among these techniques, SERS is a selectively promising technique

for detection of pesticides and thus, has been used for last two decades. With the designed SERS substrate, the considered pesticide samples concentrations well below the permissible level can be measured reliably by the Raman spectrometer.

5.2 Experimental

5.2.1 Materials

PVA of molecular weight 145000, gold beads (99.999% purity), and Malachite Green (MG) dye are purchased from Sigma-Aldrich, India. Deltamethrin, Quinalphos and Thiacloprid are acquired from local vendors. All chemicals are used as received without further processing. All the samples are prepared in DI water.

5.2.2 SERS substrate fabrication and Raman signal measurement system

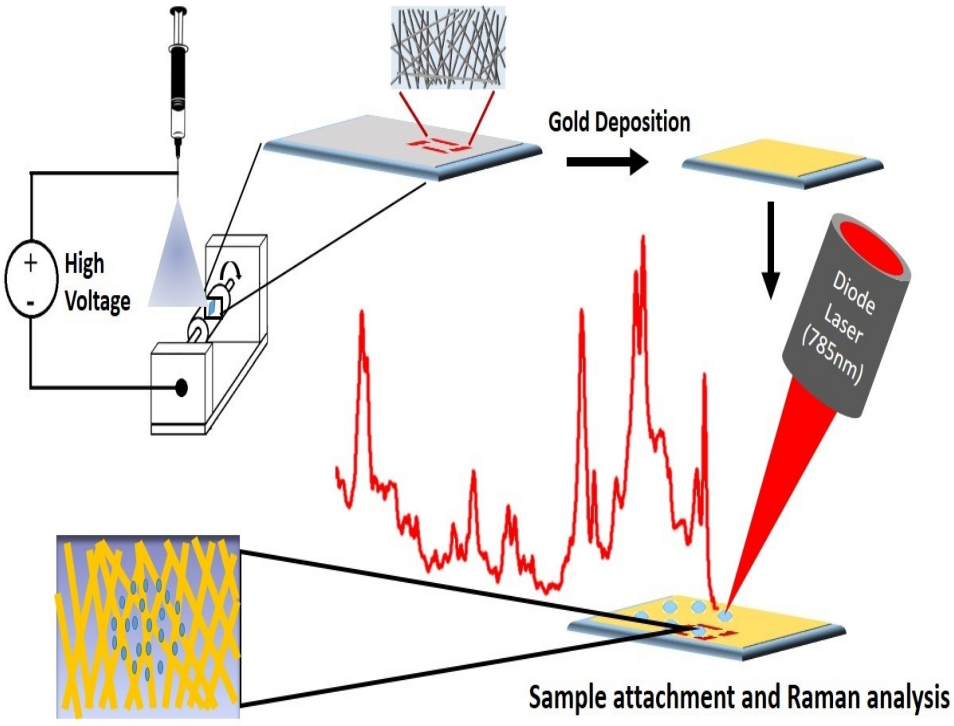

Figure 5.1: Schematic diagram of the proposed study.

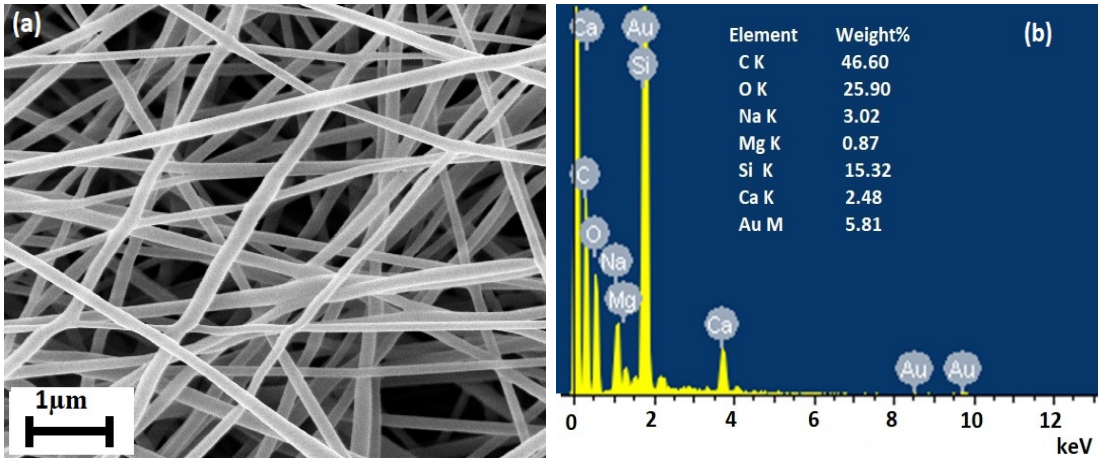

Figure 5.2: (a) FESEM image of gold coated PVA nano fibre and (b) EDX data showing the elemental compositions

Figure 5.1 shows the schematic representation of the proposed study. To fabricate the SERS substrate, initially PVA solution of 8 wt% has been prepared in DI water at 80^0C under vigorous stirring condition. Glass slides are cut into small pieces of size 1cm $\times$ 1cm. The slides are then washed under ultrasonic acetone bath followed by DI water bath and then allowed to dry in hot-air oven (Equitron Oven Ecogain Series, Media Instrument MFG Co India) at 60^0C for 1 hour. The glass slides are then mounted on a rotor by using double sided adhesion tape. The PVA nanofibers are allowed to deposit on the glass slides from an electrospinning system (ESPIN-NANO, India) for 15 minutes. During deposition of PVA nanofibers, the applied supply voltage is maintained at 16 kV, rotor speed has been set at 1500 rpm, flow rate is set at 0.3 ml/h and the mounted glass slides are kept at 15 cm away from the needle's tip. Upon deposition the nanofibers are allowed to cross-linked at 170^0C for 2 hours. Au nanofilm is deposited on these fibers using thermal evaporation technique (Hind HiVac BC300). The FESEM (Carl-Zeiss Σ IGMA VP) image of developed substrate is shown in figure 5.2 (a). The figure indicates that the diameters of the fibers are varying between 100 nm-190 nm and the spacing among the fibers are varying from few 10 nm to several 100 nm. The presence of Au in the substrate has been confirmed from the EDX data shown in figure 5.2 (b).

5.2.3 Analyte sample preparation

By dissolving proportionate amount of MG sample in DI water, 10 μM stock MG solution has been prepared in the laboratory. Required lower concentration samples are prepared by diluting the stock sample solution. Following standard procedure reported elsewhere

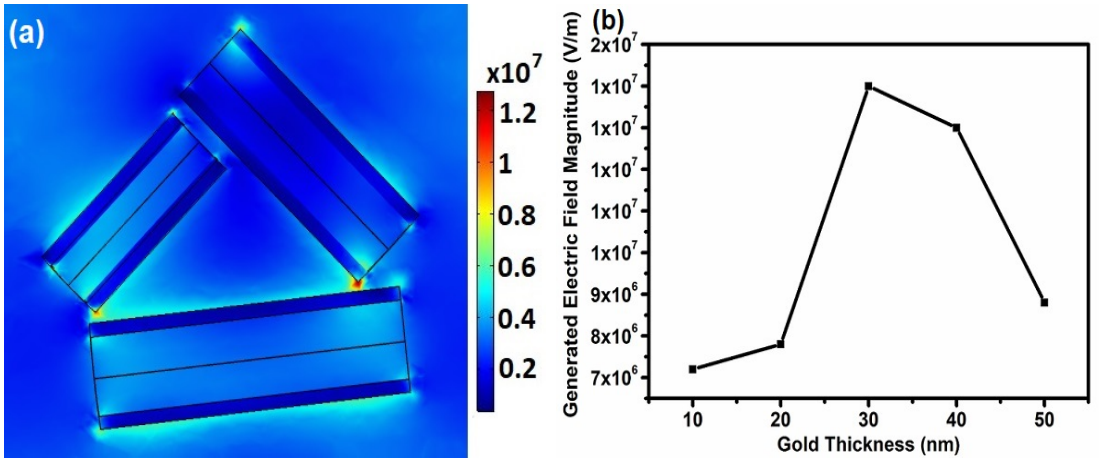

Figure 5.3: (a) Electromagnetic field distribution around the nanofiber and (b) variation generated electric field magnitude for different gold thickness when 785 nm plane polarized light is allowed to incident normally on the structure.

[36], 1 μM BPE solution has been prepared in ethanol medium. The pesticides samples are prepared by adding proportionate amount of pesticides in DI water. To record Raman signal of the considered samples, 10 μL of each of the sample is treated with the designed SERS substrate.

5.2.4 Electromagnetic (EM) simulation study

Using the simulation tool discussed in section 2.2 of chapter 2, the generated localized field magnitude has also been studied in the present work. To minimize the computational time three Au coated PVA nanofibers are considered for this study. Based on the arrangement and dimension of PVA nanofibers laid over the glass substrate, three randomly oriented PVA nanofibers of diameter 70 nm 80 nm and 100 nm have been considered on glass slide. For this study, the length of the PVA fibers are considered to be varying between 700 nm to 1000 nm and Au layer thickness is varied from 10 nm to 50 nm with a step increment of 10 nm. A plane polarized light of wavelength 785 nm is allowed to incident normally on the designed structure. The generated EM field magnitude around the fibers is shown in figure 5.3 (a). For the designed pattern, maximum field magnitude of 1.23×10^7 V/m has been observed. Figure 5.3 (b) illustrates the maximum field coupling conditions for different Au film thickness on the substrate. These simulation results reveal that with 30 nm thick Au layer, the proposed substrate yields the maximum field coupling condition when it is illuminated with 785 nm laser source.

5.3 Results and Discussions

5.3.1 Characterization of the substrate

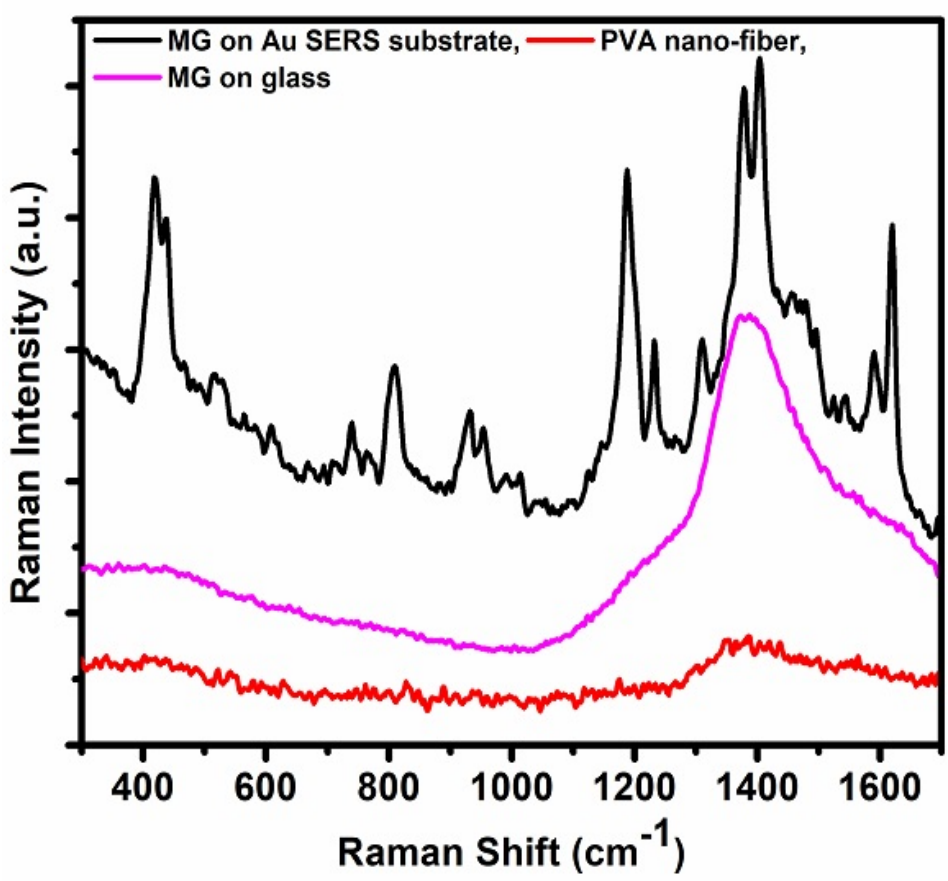

Figure 5.4: A comparison of Raman signal of MG scattered from three different substrates namely plane glass substrate, PVA nanofiber coated substrate and gold coated PVA nanofiber substrate.

Initially, the performance of the designed SERS substrate is evaluated using MG as an analyte sample. 10 μL of 10 μM MG sample is pipetted on the developed SERS substrate. Same volume of the sample solution is also treated with a plane glass substrate and on bare PVA nanofiber deposited glass substrate. All the sample treated substrates are allowed to dry for 2 hours at room temperature. Upon drying of the sample, Raman signal from the sample is recorded by the Raman spectrometer for all the three different substrates. Figure 5.4 illustrates the characteristic Raman spectrum of MG scattered from the designed SERS substrate and from the other considered substrates. Clearly, the figure depicts that the substrate with Au coated PVA nanofiber scatters strong Raman signal compared to plane glass substrate and bare PVA nanofibers. The bond assignments of the signature peaks of MG has already been discussed in section 3.3.1 in chapter 3.

Effect of Au film thickness on Raman signal enhancement

The thickness of Au film on PVA nanofiber could influence the overall Raman signal intensity. In order to study how Au nanofilm thickness effects on Raman signal intensity, three substrates with Au film thickness 10 nm, 30 nm and 60 nm have been prepared. The substrates are then treated with 10 μM MG solution and back scattered Raman signals from these substrates are recorded from 6 different locations on each substrate. Figure 5.5 shows the variation of average signature peak signal intensity at 1188 cm^{-1} for the considered substrates. Among the considered Au films, the highest Raman signal intensity is observed for the substrate with 30 nm Au nanofilm. This experimental result is supported by the simulation study discussed in section 5.2.4 in this chapter.

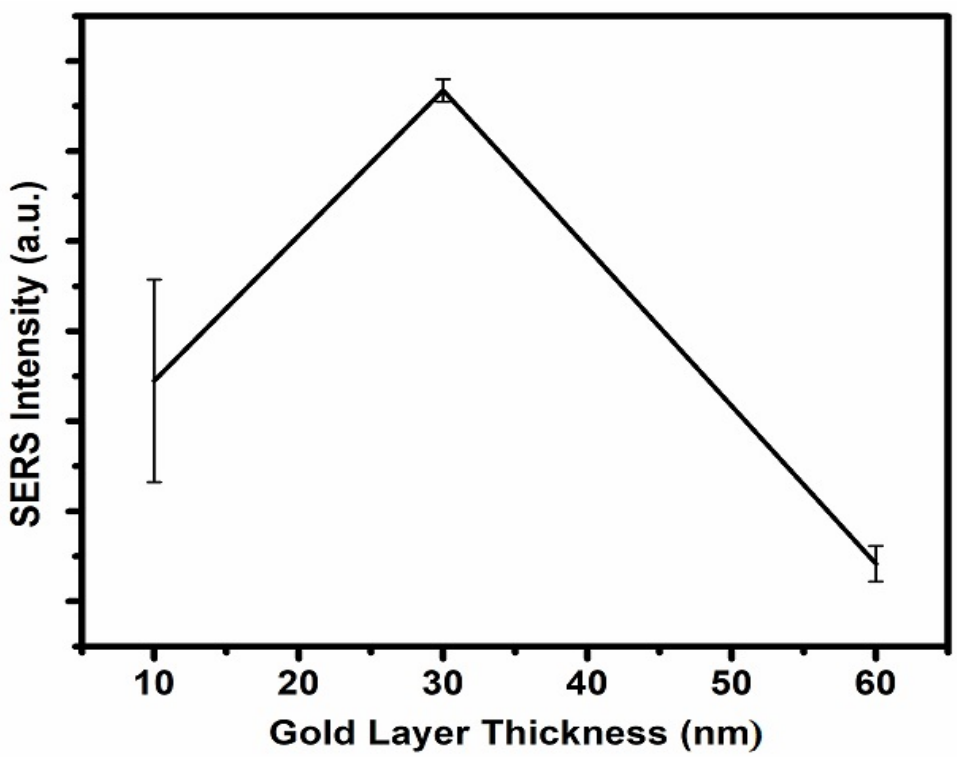

Figure 5.5: Characteristics curve of variation of scattered Raman signal intensity of MG at 1188 cm^{-1} with the variation of deposited gold layer thickness.

Minimum measurable sample concentration and EF estimation

Three more MG samples with concentrations 1 μM, 100 nM and 10 nM have been prepared by diluting the stock sample. After treatment of the sample solutions separately with the proposed SERS substrate, the back-scattered Raman signals of these samples are recorded by the Raman spectrometer. The characteristic Raman signals intensity variation of different concentration MG samples scattered from the substrates are shown in figure 5.6. Clearly, from the figure, it is seen that the peak Raman signal intensities decrease gradually with the decrement of MG concentration. With the proposed SERS substrate minimum concentration of 10 nM can be measured reliably by the spectrometer. To estimate the EF of the substrate, again equation 1.22 has been used. Raman peak

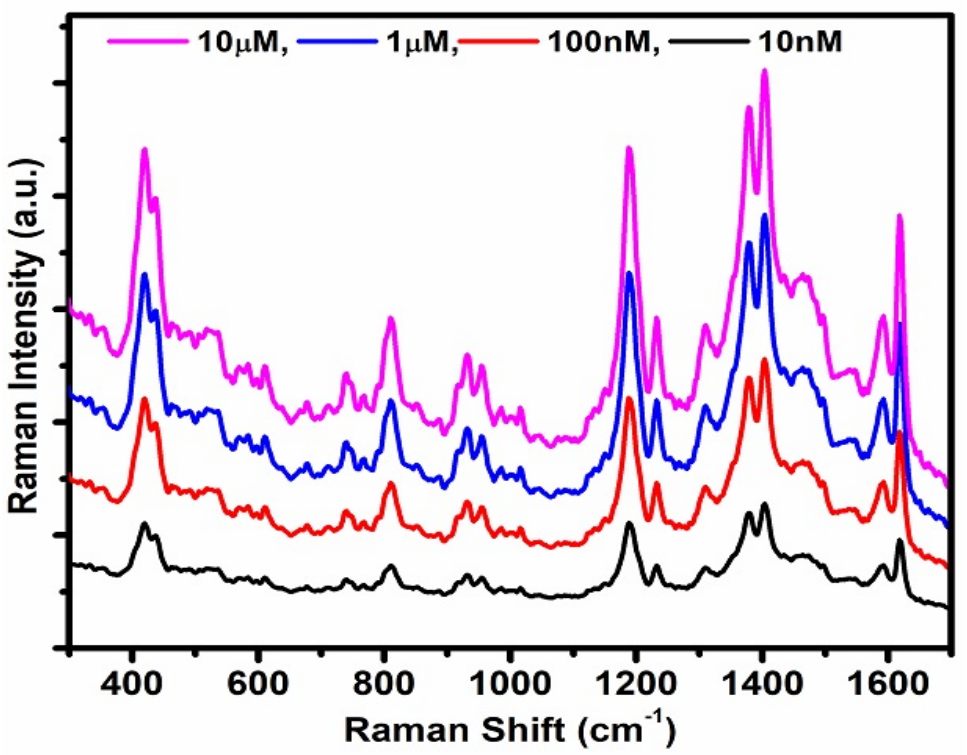

Figure 5.6: Raman signal scattered from developed SERS substrate while different concentrations 10 μM, 1 μM, 100 nM and 10 nM of MG solution are tested.

intensities of MG at 1188 cm^{-1}, I_{SERS} and I_{REF} value are observed to be 3321 a.u. and 224 a.u. respectively. Considering uniform distribution of the analyte molecules over the reference substrate, N_{REF} is calculated to be 4.40×10^7 for laser spot size dimension of 4.35 μm. Considering monolayer distribution of MG sample over the developed substrate, the N_{SERS} is calculated to be 4.40×10^2. The average field EF at 1188 cm^{-1} of MG is estimated to be 1.48×10^6.

Reproducibility and spectral uniformity of the substrate

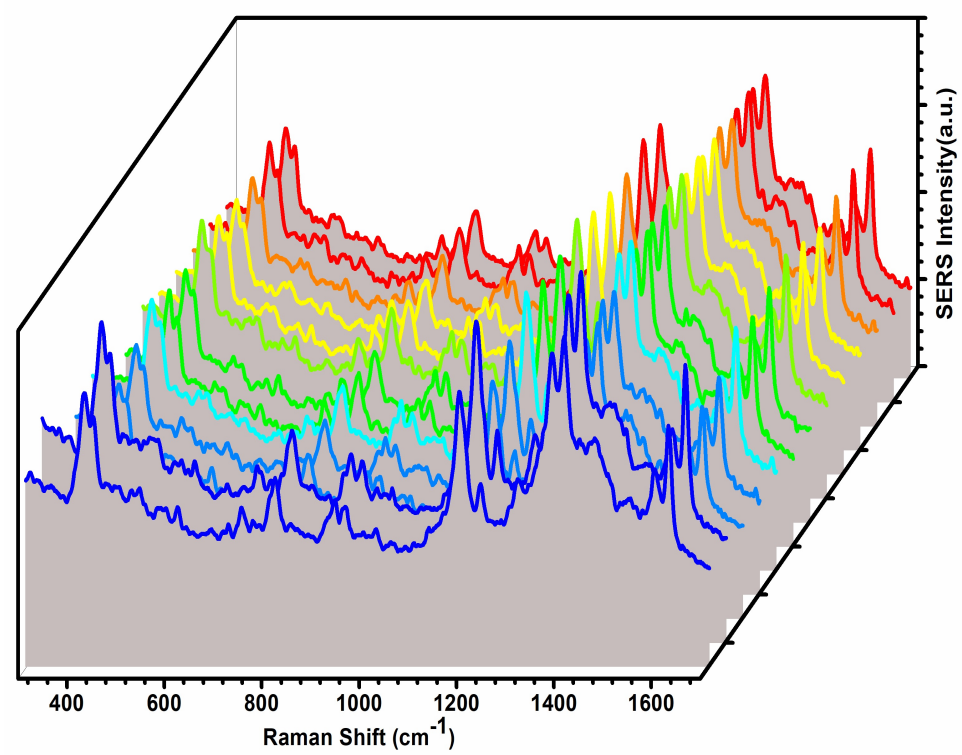

Figure 5.7: Back scattered Raman signal intensities of 10 μM MG recorded from 13 different locations of the proposed substrate.

To study the reproducibility characteristic of the proposed SERS substrate, back scattered Raman signals have been recorded from 13 different randomly selected locations of 10 μM MG treated SERS substrate. Figure 5.7 depicts the characteristic Raman spectra of the sample measured from these locations. The Raman peaks intensities of MG at 420 cm^{-1}, 1188 cm^{-1}, 1378 cm^{-1} and 1618 cm^{-1} are observed to be varying in 6.01%, 7.38%, 5.71% and 6.50% respectively. The low peak intensity fluctuations of this sample suggest that the proposed SERS substrate is highly reproducible.

In the present study, the incident laser spot covers an analyzing area of 14.88 μm^2 over the SERS substrate. The relatively wider analyzing area of the sensing region of SERS substrate provides an average Raman signal enhancement information from the sensing region of the substrate. Thus, even though the PVA nanofibers are oriented in random directions, due to the consideration of average field enhancement over a relatively large area, reasonably good reproducibility of the designed substrate has been noticed.

To evaluate the spectral uniformity characteristics of the substrate for a non-fluorescent Raman active sample- 1,2-bis(4-pyridyl)ethylene (BPE) has been used. The BPE solution of concentration 1 μM has been treated with the substrate and allowed to dry. Upon drying of the sample, the back-scattered Raman signals of BPE are measured by mapping

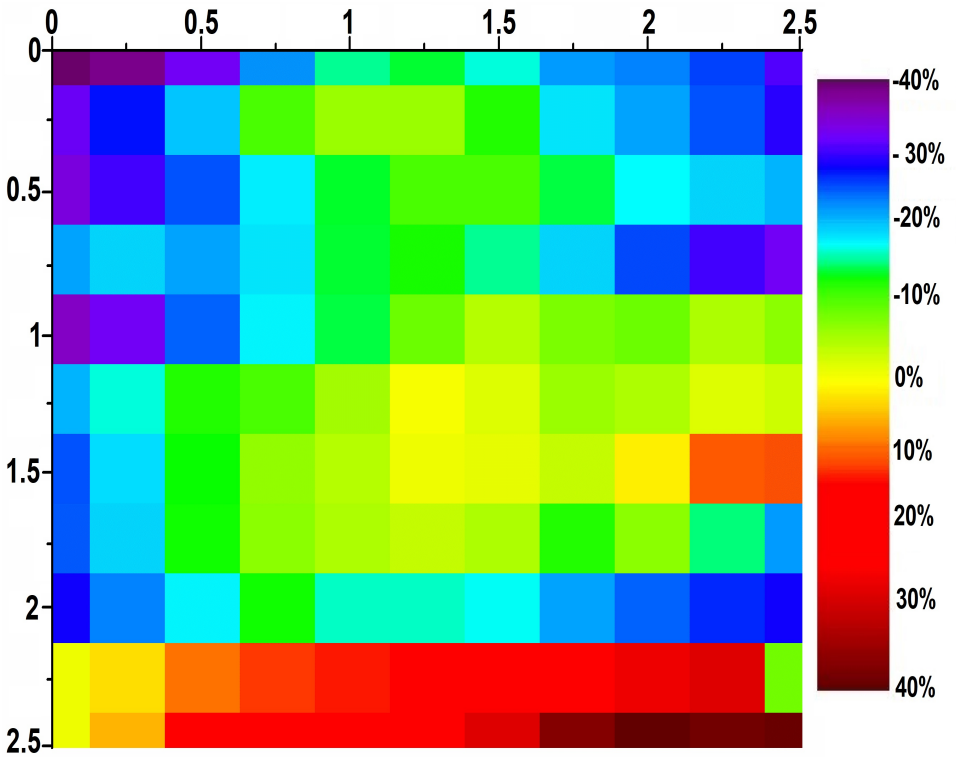

Figure 5.8: Raman Signal intensity variation scattered from different locations of the substrate at wavenumber 1214 cm^{-1} when BPE is functionalized with the substrate, the mapping is done over an area of 2.5 mm × 2.5 mm.

it over an area of 2.5 mm×2.5 mm with an array of 11×11. Figure 5.8 shows the intensity variation Raman signal of BPE at 1214 cm^{-1} over the considered mapping region of the SERS substrate. The maximum SERS signal intensity is observed to be varying by 40%, however, over 80% of the mapping area, the intensity fluctuation is found to be below 20%, which again signifies a good degree of spectral uniformity of the proposed SERS substrate.

Life span evaluation of the SERS substrate

To evaluate the durability of the substrate, Raman signal from MG treated substrates has been recorded for 30 days. The maximum intraday peak intensity fluctuations is observed to be 8.54% and maximum intensity fluctuations from the average value during the investigation period is found to be 10.56% corresponding to the signature Raman peak at 1186 cm^{-1}. This indicates a good life span and stability of the substrate. Figure 5.9 illustrates the characteristic stability response of the proposed SERS substrate while considering MG as test sample and has been observed for 30 days.

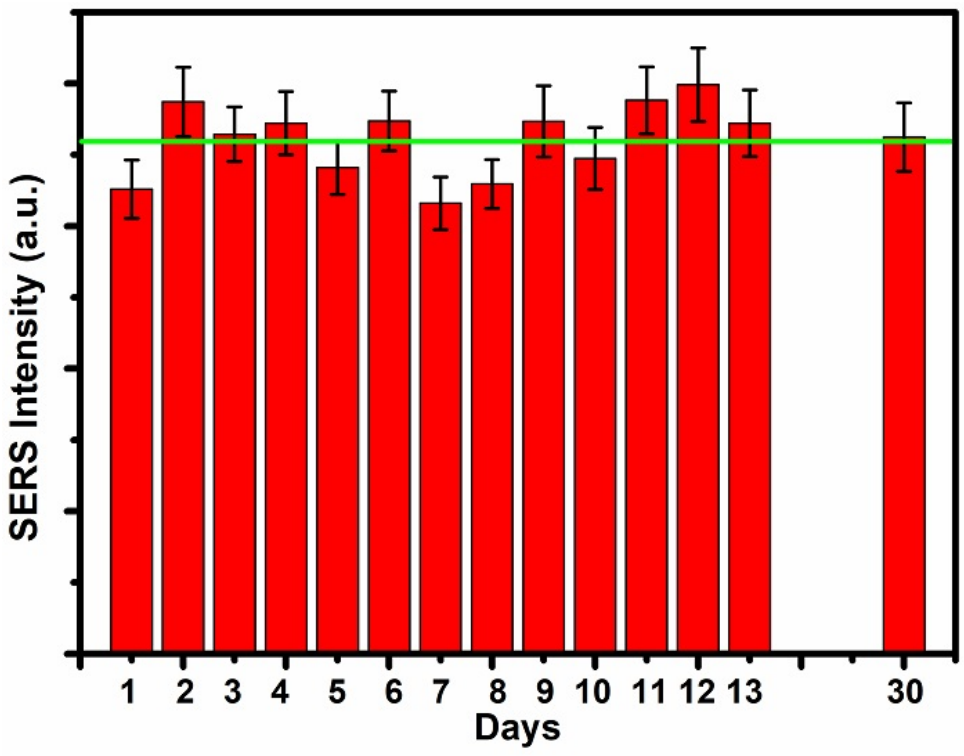

Figure 5.9: Stability study of the proposed SERS substrate through investigating the intensity fluctuations of Raman peak (1188 cm^{-}1) for 1 μM MG treated on it for 30 days.

Estimation of LoD

In the next step of the present work, the limit of detection (LoD) of the proposed SERS substrate has been estimated using MG as test sample. In order to evaluate this parameter 5 different concentration of MG- 20 nM (0.00734 mg/L), 40 nM (0.01467 mg/L), 60 nM (0.02201 mg/L), 80 nM (0.01935 mg/L) and 100 nM (0.03669 mg/L) have been prepared and treated separately with the proposed substrates. Raman signals from each substrate are recorded from 7 randomly selected locations. Figure 5.10 indicates the normalized SERS signal intensity variations of MG corresponding to Raman peak positioned at 1188 cm^{-1}. The LoD has been calculated using equation 5.1 [37].

$$LoD = \frac{3.3\sigma}{S} \tag{5.1}$$

where σ is the standard deviation of y-intercepts and S is the slope of the linear fitted line. For MG the LoD of the design substrate is calculated to be 0.01148 mg/L.

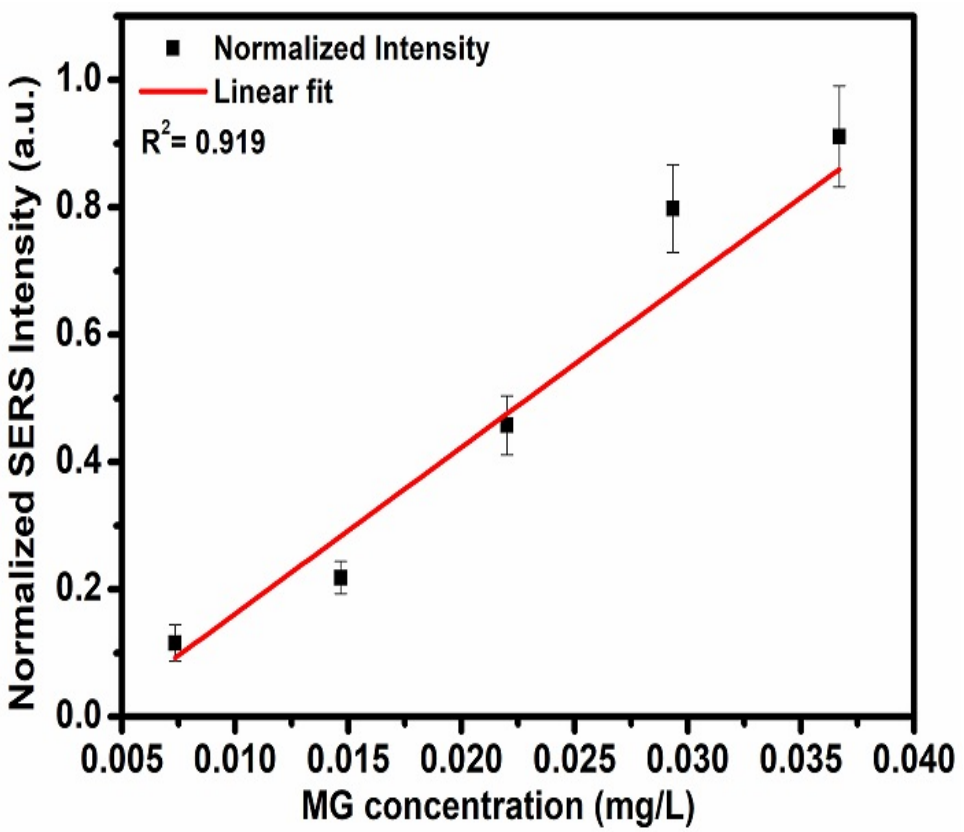

Figure 5.10: Normalized SERS signal intensity variation of MG solution corresponding to Raman peak 1188 cm^{-1} for the concentrations 0.00734 mg/L to 0.03669 mg/L.

5.3.2 Detection of pesticides

In the final step of the present study, the applicability of the proposed SERS substrate for detection of three commonly used pesticides- deltamethrin, quinalphos and thiacloprid have been demonstrated. Pesticides residues cause pollution in the environment and are hazardous to human health. A series of studies to detect minimum concentration of considered pesticide samples by the Raman spectrometer upon its treatment with the proposed SERS substrate have been carried out. Deltamethrin is generally used in crop, gardens, lawns etc. as an insects repellent. Though there are no reported cases of acute health issue from deltamethrin yet, it is highly toxic for aquatic environment [38-40]. Quinalphos is widely used in several developing and underdeveloped nations for better yield of the crops namely wheat, rice, maize, coffee, sugarcane, cotton etc. Excessive content (more than 0.5 mg/kg body weight) of this chemical in food items may cause toxicity which includes carcinogenicity, reproductive and developmental toxicity, neurotoxicity. It is listed as moderate toxic chemical by world health organization (WHO) and use of this pesticide is restricted in several nations [41]. Again thiacloprid is used

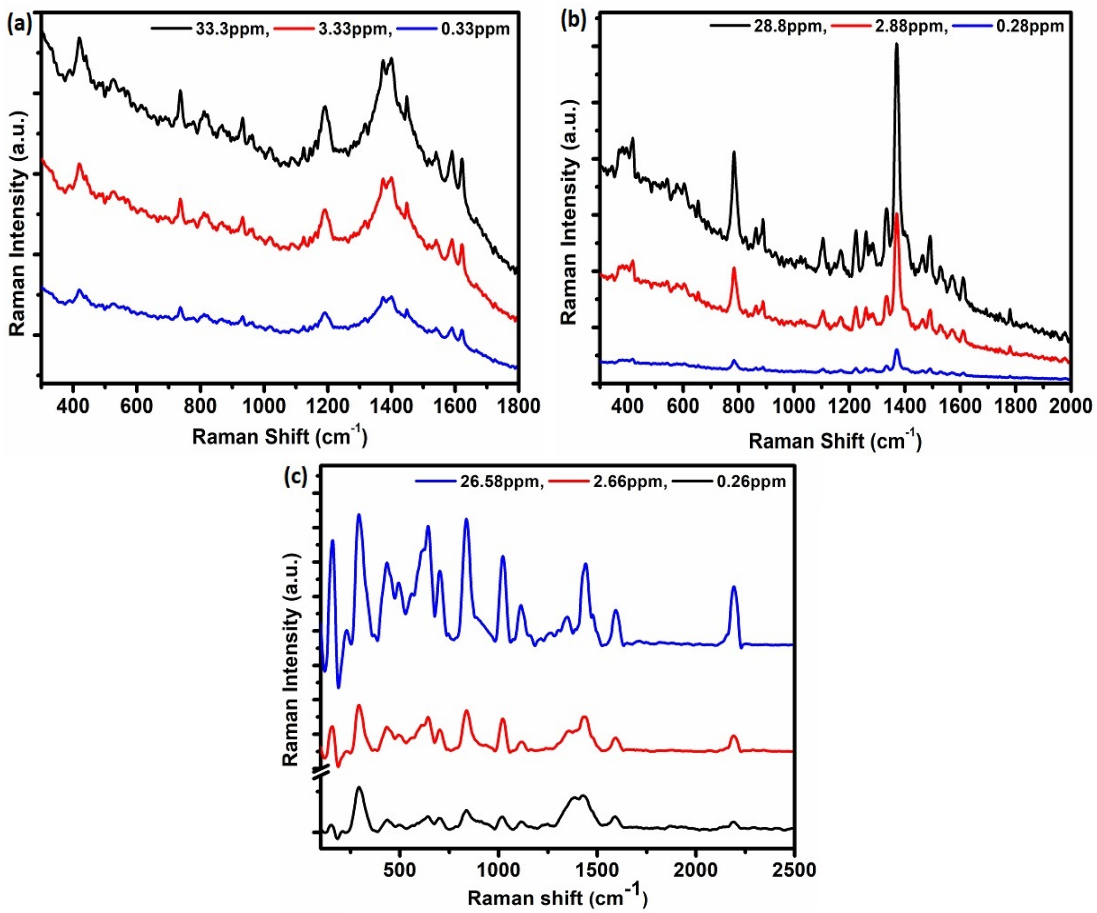

Figure 5.11: Raman signal of (a) Deltamethrin, (b) Quinalphos and (c) Thiacloprid at different concentration level scattered from the developed SERS substrate upon functionalization of the pesticides.

in crop fields and gardens also as an insect repellent. Direct exposer of this pesticide may cause skin and eye irritation. The maximum permissible limits of use of these pesticides in agriculture and food materials can be found elsewhere [42]. Three different concentrations of the pesticides sample are prepared in the laboratory and then treated with the SERS substrate separately. The recorded Raman signals for deltamethrin are shown in figure 5.11 (a). The characteristics Raman peaks of deltamethrin are observed at 736 cm^{-1}, 1192 cm^{-1}, 1400 cm^{-1}, 1448 cm^{-1}, 1590 cm^{-1} and 1622 cm^{-1} which are attributed to C-Br stretching, C-O-C stretching of ether group, CH_3 deformation, CH_3 anti-symmetric deformation, aromatic benzene ring stretching and C=O stretch of phenol ether respectively. These characteristic peaks can be clearly visible even after diluting the sample to 0.33 ppm. The SERS spectra for quinalphos is shown in figure 5.11 (b). Very sharp and strong peak is observed at 1370 cm^{-1} which corresponds to CH_3 symmetric deformation. Other peaks at 784 cm^{-1}, 1224 cm^{-1}, 1260 cm^{-1}, 1490 cm^{-1} and 1780 cm^{-1} are attributed to CH out of plane deformation, C-C-N bending, C-N stretching,

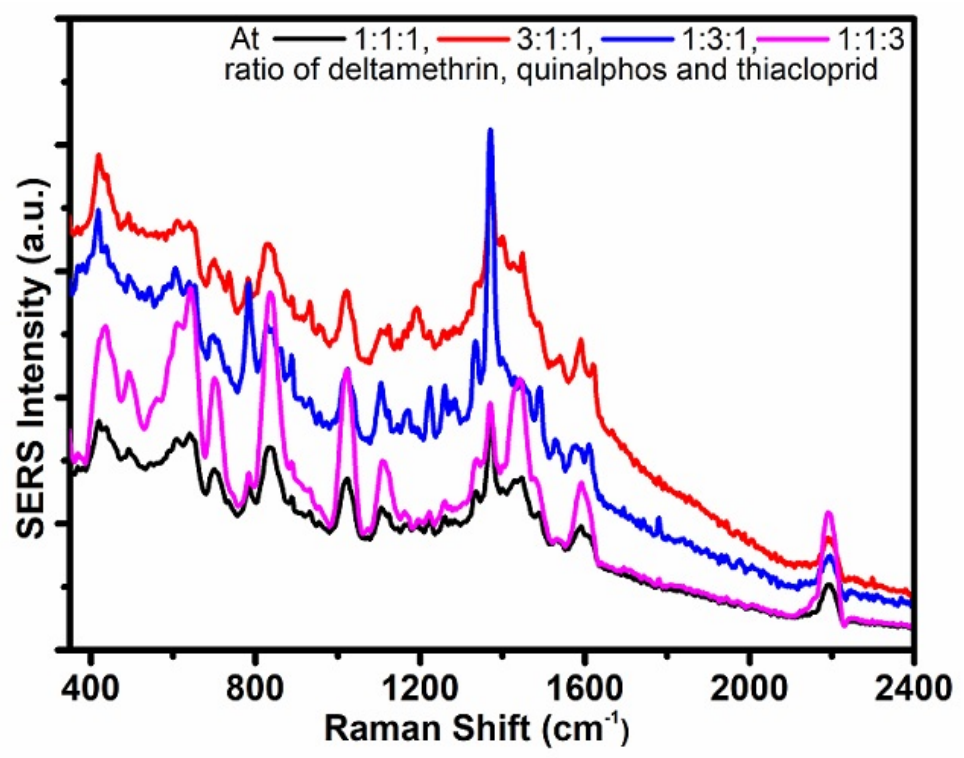

Figure 5.12: Raman signal intensity of deltamethrin, quinalphos and thiacloprid mixture when these are mixed at different ratio.

ring stretching and C=O stretching respectively. The Raman signals for this specific pesticide are measurable even when the concentration of the sample has been reduced to 0.28 ppm. Figure 5.11 (c) illustrates the characteristics SERS spectra of different concentrations of thiacloprid sample. Signature Raman peaks at 434 cm^{-1} and 644 cm^{-1} are observed due to bending of C-N-C and C-S stretching while 702 cm^{-1} and 836 cm^{-1} correspond to stretching of C-Cl bond. Again 1024 cm^{-1}, 1112 cm^{-1}, 1440 cm^{-1} and 1594 cm^{-1} peaks are observed due to ring breathing mode, C-N stretching, scissors vibration of CH_2 and C=C stretching respectively. With the designed SERS substrate thiacloprid concentration as low as 0.26 ppm can be detected reliably. Table 5.1 summarizes the maximum permissible limit of the above pesticide samples set by USDA and the minimum concentrations of these samples which can be detected by the present technique. The table also contains the minimum detectable concentrations of these samples by other techniques. Clearly, for all the pesticides samples considered in the present study, one can record the Raman signals of the samples well below the permissible limit with the proposed SERS substrate.

Table 5.1: Comparison between maximum residue limit of the considered pesticides and minimum detectable concentration of developed SERS substrate.

Pesticides	**Maximum permissible residue limit (mg/Kg) (USDA report)**	**Minimum detectable concentration with the proposed SERS substrate (mg/Kg)**	**LoD of other techniques**	**Remark**
Deltamethrin	10.00	0.33	<1 ng/mL [43]	Used in rice, wheat, pea, cabbage, broccoli, sweet potato, olive, tea etc. can be detected reliably
Quinalphos	0.50	0.288	5.5 mg/Kg [44]	Used in citrus fruits. Can be detect reliably
Thiacloprid	1.00	0.2658	1.8 ng/mL [45]	Used in mustard seed, tomato, cucumber, barriers etc. and can be detected reliably

Multimodal sensing

In order to evaluate the multimodal sensing characteristic of the proposed SERS substrate, four more samples have been prepared by mixing deltamethrin: quinalphos: thiacloprid in the ratio 1:1:1, 3:1:1, 1:3:1 and 1:1:3. The mixtures have been treated separately with the substrates. Figure 5.12 shows the characteristics Raman signals for different combination of pesticides samples in the mixture. The figure indicates that when all the pesticides are mixed in equal proportion the strong Raman peaks of each of the pesticide sample can be observed. For instance, when the pesticides are mixed in the ratio 1:1:1, the strong Raman peaks of deltamethrin at 1590 cm^{-1}, for quinalphos at 1370 cm^{-1} and at 836 cm^{-1} for thiacloprid can be distinctly observed. These characteristics Raman peaks intensities are found to be increased proportionately with the increase in composition of the respective pesticide in the mixture. This study suggests that with the proposed SERS substrate, the pesticides samples can be specifically recorded and analyzed in the mixture.

5.4 Summary

A technique to obtain low-cost, fairly reproducible and sensitive SERS substrate using electrospinning technique has been demonstrated. MG concentration as low as 10 nM can be detected with the proposed SERS substrate. An average EF of the order of 1.48×10^6 has been observed corresponding to the signature peak of MG at 1188 cm^{-1}. For the designed SERS substrate the simulation results yield a local field enhancement of 2.06×10^2, thus providing an average SERS EF of the order 10^9. However, MG as analyte sample treated over the substrate the average EF is found to be 10^6. The experimentally low EF value of the designed SERS substrate is attributed to the random distribution of PVA nanofibers over the glass substrate, which might cause a different magnitude of the coupled electromagnetic field at different points over the sensing region of the SERS substrate. The developed substrate shows consistent result over a period of 30 Days. LoD of the substrate is calculated to be 0.01148 mg/L while using MG as a test sample. Using the proposed SERS substrate detection and analysis of three commonly used pesticides namely deltamethrin, quinalphos and thiacloprid have been successfully demonstrated. Minimum concentrations of deltamethrin, quinalphos and thiacloprid that can be detected with the developed substrate are 0.33 ppm, 0.28 ppm and 0.26 ppm respectively. All these detectable concentrations are well below the permissible limit as set in the global agricultural information network (GAIN) report from United States Department of agriculture (USDA), foreign agricultural service. The SERS substrate can be fabricated without the requirement of sophisticated instruments and laboratory facility. It is envisioned that the designed SERS substrate could potentially emerge as a low-cost Raman signal sensing platform for reliable detection and quantification of other chemicals and biological samples.

References

[1] Chou, S.-Y., Yu, C.-C., Yen, Y.-T., Lin, K.-T., Chen, H.-L., and Su, W.-F. Romantic story or Raman scattering? rose petals as ecofriendly, low-cost substrates for ultrasensitive surface-enhanced Raman scattering. *Analytical chemistry,* 87(12):6017-6024, 2015.

[2] Xu, B.-B., Zhang, Y.-L., Zhang, W.-Y., Liu, X.-Q., Wang, J.-N., Zhang, X.-L., Zhang, D.-D., Jiang, H.-B., Zhang, R., and Sun, H.-B. Silver-coated rose petal: green, facile, low-cost and sustainable fabrication of a SERS substrate with unique superhydrophobicity and high efficiency. *Advanced Optical Materials,* 1(1):56-60, 2013.

[3] Yang, J., Zhen, L., Ren, F., Campbell, J., Rorrer, G. L., and Wang, A. X. Ultrasensitive immunoassay biosensors using hybrid plasmonic-biosilica nanostructured materials. *Journal of biophotonics,* 8(8):659-667, 2015.

[4] Ren, F., Campbell, J., Rorrer, G. L., andWang, A. X. Surface-enhanced Raman spectroscopy sensors from nanobiosilica with self-assembled plasmonic nanoparticles. *IEEE Journal of Selected Topics in Quantum Electronics,* 20(3):127-132, 2014.

[5] Kumar, P., Khosla, R., Soni, M., Deva, D., and Sharma, S. K. A highly sensitive, flexible SERS sensor for malachite green detection based on Ag decorated microstructured PDMS substrate fabricated from taro leaf as template. *Sensors and Actuators B: Chemical,* 246:477-486, 2017.

[6] Yu, W. W. and White, I. M. Inkjet printed surface enhanced Raman spectroscopy array on cellulose paper. *Analytical chemistry,* 82(23):9626-9630, 2010.

[7] Liao, W.-J., Roy, P. K., and Chattopadhyay, S. An ink-jet printed, surface enhanced raman scattering paper for food screening. *RSC Advances,* 4(76):40487-40493, 2014.

[8] Wu, W., Liu, L., Dai, Z., Liu, J., Yang, S., Zhou, L., Xiao, X., Jiang, C., and Roy, V. A. Low-cost, disposable, flexible and highly reproducible screen printed SERS substrates for the detection of various chemicals. *Scientific reports,* 5:10208, 2015.

[9] Gaaz, T. S., Sulong, A. B., Akhtar, M. N., Kadhum, A. A. H., Mohamad, A. B., and Al-Amiery, A. A. Properties and applications of polyvinyl alcohol, halloysite nanotubes and their nanocomposites. *Molecules,* 20(12):22833-22847, 2015.

[10] Kim, C.-K., Kim, B.-S., Sheikh, F. A., Lee, U.-S., Khil, M.-S., and Kim, H.-Y. Amphiphilic poly (vinyl alcohol) hybrids and electrospun nanofibers incorporating polyhedral oligosilsesquioxane. *Macromolecules,* 40(14):4823-4828, 2007.

[11] Park, J.-C., Ito, T., Kim, K.-O., Kim, K.-W., Kim, B.-S., Khil, M.-S., Kim, H.-Y., and Kim, I.-S. Electrospun poly (vinyl alcohol) nanofibers: effects of degree of hydrolysis and enhanced water stability. *Polymer journal,* 42(3):273, 2010.

[12] Shafiee, A., Soleimani, M., Chamheidari, G. A., Seyedjafari, E., Dodel, M., Atashi, A., and Gheisari, Y. Electrospun nanofiber-based regeneration of cartilage enhanced by mesenchymal stem cells. *Journal of biomedical materials research Part A,* 99(3):467-478, 2011.

[13] Das, P., Ojah, N., Kandimalla, R., Mohan, K., Gogoi, D., Dolui, S. K., and Choudhury, A. J. Surface modification of electrospun PVA/chitosan nanofibers by dielectric barrier discharge plasma at atmospheric pressure and studies of their mechanical properties and biocompatibility. *International journal of biological macromolecules,* 114:1026-1032, 2018.

[14] Majd, S. A., Khorasgani, M. R., Moshtaghian, S. J., Talebi, A., and Khezri, M. Application of chitosan/PVA nano fiber as a potential wound dressing for streptozotocin-induced diabetic rats. *International journal of biological macromolecules,* 92:1162-1168, 2016.

[15] Baca, A. S., Bryhan, M. D., Noll, F. E., Petzold, O. N., Price, M. W., Senaratne, W., and Walczak, W. J. Nanofibers, nanofilms and methods of making/using thereof, 2008. *US Patent App.* 11/899,589.

[16] Gradess, R., Abargues, R., Habbou, A., Canet-Ferrer, J., Pedrueza, E., Russell, A., Valdées, J. L., and Martínez-Pastor, J. P. Localized surface plasmon resonance sensor based on Ag-PVA nanocomposite thin films. *Journal of Materials Chemistry,* 19(48):9233-9240, 2009.

[17] Filippo, E., Serra, A., and Manno, D. Poly (vinyl alcohol) capped silver nanoparticles as localized surface plasmon resonance-based hydrogen peroxide sensor. *Sensors and Actuators B: Chemical,* 138(2):625-630, 2009.

[18] Arias-Estévez, M., López-Periago, E., Martínez-Carballo, E., Simal-Gándara, J., Mejuto, J.-C., and García-Río, L. The mobility and degradation of pesticides in soils and the pollution of groundwater resources. *Agriculture, Ecosystems & Environment,* 123(4):247-260, 2008.

[19] Aktar, W., Sengupta, D., and Chowdhury, A. Impact of pesticides use in agriculture: their benefits and hazards. *Interdisciplinary toxicology,* 2(1):1-12, 2009.

[20] Pesticide residues in food Fact sheet, WHO, http://www.who.int/mediacentre/factsheets/pesticide-residues-food/en/2017 July

[21] Damalas, C. A. and Eleftherohorinos, I. G. Pesticide exposure, safety issues, and risk assessment indicators. *International journal of environmental research and public health,* 8(5):1402-1419, 2011.

[22] Lehotay, S. J., Kok, A. d., Hiemstra, M., and Bodegraven, P. v. Validation of a fast and easy method for the determination of residues from 229 pesticides in fruits and vegetables using gas and liquid chromatography and mass spectrometric detection. *Journal of AOAC International,* 88(2):595-614, 2005.

[23] Berijani, S., Assadi, Y., Anbia, M., Hosseini, M.-R. M., and Aghaee, E. Dispersive liquid-liquid microextraction combined with gas chromatography-flame photometric detection: very simple, rapid and sensitive method for the determination of organophosphorus pesticides in water. *Journal of Chromatography A,* 1123(1):1-9, 2006.

[24] Van der Hoff, G. R. and van Zoonen, P. Trace analysis of pesticides by gas chromatography. *Journal of Chromatography A,* 843(1-2):301-322, 1999.

[25] Nunez, O., Moyano, E., and Galceran, M. T. LC-MS/MS analysis of organic toxics in food. *TrAC Trends in Analytical Chemistry,* 24(7):683-703, 2005.

[26] Rial-Otero, R., Gaspar, E., Moura, I., and Capelo, J. Chromatographic-based methods for pesticide determination in honey: An overview. *Talanta,* 71(2):503-514, 2007.

[27] Cheng, X., Wang, Q., Zhang, S., Zhang, W., He, P., and Fang, Y. Determination of four kinds of carbamate pesticides by capillary zone electrophoresis with amperometric detection at a polyamide-modified carbon paste electrode. *Talanta,* 71(3):1083-1087, 2007.

[28] Barcelo, D., Durand, G., Bouvot, V., and Nielen, M. Use of extraction disks for trace enrichment of various pesticides from river water and simulated seawater samples followed by liquid chromatography-rapid-scanning UV-visible and thermospray-mass spectrometry detection. *Environmental science & technology,* 27(2):271-277, 1993.

[29] Xiong, D. and Li, H. Colorimetric detection of pesticides based on calixarene modified silver nanoparticles in water. *Nanotechnology,* 19(46):465502, 2008.

[30] Meulenberg, E. P., Mulder, W. H., and Stoks, P. G. Immunoassays for pesticides. *Environmental science & technology,* 29(3):553-561, 1995.

[31] Lisa, M., Chouhan, R., Vinayaka, A., Manonmani, H., and Thakur, M. Gold nanoparticles based dipstick immunoassay for the rapid detection of dichlorodiphenyltrichloroethane: an organochlorine pesticide. *Biosensors and Bioelectronics,* 25(1):224-227, 2009.

[32] Chand, S., Gupta, B., et al. Surface plasmon resonance based fiber-optic sensor for the detection of pesticide. *Sensors and Actuators B: Chemical,* 123(2):661-666, 2007.

[33] Yang, J.-K., Kang, H., Lee, H., Jo, A., Jeong, S., Jeon, S.-J., Kim, H.-I., Lee, H.-Y., Jeong, D. H., Kim, J.-H., et al. Single-step and rapid growth of silver nanoshells as SERS-active nanostructures for label-free detection of pesticides. *ACS applied materials & interfaces,* 6(15):12541-12549, 2014.

[34] Kumar, S., Goel, P., and Singh, J. P. Flexible and robust SERS active substrates for conformal rapid detection of pesticide residues from fruits. *Sensors and Actuators B: Chemical,* 241:577-583, 2017.

[35] Zacco, E., Pividori, M. I., Alegret, S., Galvée, R., and Marco, M.-P. Electrochemical magnetoimmunosensing strategy for the detection of pesticides residues. *Analytical chemistry,* 78(6):1780-1788, 2006.

[36] Xu, Z., Jiang, J., Wang, X., Han, K., Ameen, A., Khan, I., Chang, T.-W., and Liu, G. L. Large-area, uniform and low-cost dual-mode plasmonic naked-eye colorimetry and SERS sensor with handheld raman spectrometer. *Nanoscale,* 8(11):6162-6172, 2016.

[37] Guideline, I. H. T. Validation of analytical procedures: text and methodology q2 (r1). In *International Conference on Harmonization, Geneva, Switzerland,* 11-12. 2005.

[38] Balint, T., Szegletes, T., Szegletes, Z., Halasy, K., and Nemcsok, J. Biochemical and subcellular changes in carp exposed to the organophosphorus methidathion and the pyrethroid deltamethrin. *Aquatic Toxicology,* 33(3-4):279-295, 1995.

[39] Viran, R., Erkoç, F. Ü., Polat, H., and Koçak, O. Investigation of acute toxicity of deltamethrin on guppies (poecilia reticulata). *Ecotoxicology and environmental safety,* 55(1):82-85, 2003.

[40] Angahar, L. Investigations of acute toxicity and neurotoxin effects of aqueous extracted pyrethroid (deltamethrin) from insecticide treated mosquito net on clarias gariepinus and heterobranchus bidorsalis. moj biol med 1 (4): 00020, 2017.

[41] Kegley, S., Hill, B., Orme, S., and Choi, A. Pan pesticide database. *Pesticide Action Network, North America (San,* 2000.

[42] USDA foreign agricultural service, G. r. Maximum residue limits for pesticides in food. https://gain.fas.usda.gov/Recent, 2014.

[43] Liu, X., Li, L., Liu, Y.-Q., Shi, X.-B., Li, W.-J., Yang, Y., and Mao, L.-G. Ultrasensitive detection of deltamethrin by immune magnetic nanoparticles separation coupled with surface plasmon resonance sensor. *Biosensors and Bioelectronics,* 59:328-334, 2014.

[44] Hu, H., Liu, X., Jiang, F., Yao, X., and Cui, X. A novel chemiluminescence assay of organophosphorous pesticide quinalphos residue in vegetable with luminol detection. *Chemistry Central Journal,* 4(1):13, 2010.

[45] Liu, Z. J., Wei, X., Xu, H., Li, M., Zhu, G. B., Xue, Y. L., Zhang, Z., Zhao, G. D., and Du, D. L. Sensitive detection of thiacloprid in environmental and food samples by enhanced chemiluminescent enzyme immunoassay. *RSC Advances,* 6(35):29460-29465, 2016.